



Deposited via The University of Leeds.

White Rose Research Online URL for this paper:

<https://eprints.whiterose.ac.uk/id/eprint/169758/>

Version: Accepted Version

Article:

Stana, R, Lythe, G and Molina-Paris, C (2021) Diffusion in a Disk with a Circular Inclusion. SIAM Journal on Applied Mathematics, 81 (3). pp. 1287-1302. ISSN: 0036-1399

<https://doi.org/10.1137/20M1351394>

Reuse

Items deposited in White Rose Research Online are protected by copyright, with all rights reserved unless indicated otherwise. They may be downloaded and/or printed for private study, or other acts as permitted by national copyright laws. The publisher or other rights holders may allow further reproduction and re-use of the full text version. This is indicated by the licence information on the White Rose Research Online record for the item.

Takedown

If you consider content in White Rose Research Online to be in breach of UK law, please notify us by emailing eprints@whiterose.ac.uk including the URL of the record and the reason for the withdrawal request.

DIFFUSION IN A DISK WITH A CIRCULAR INCLUSION

REMUS STANA, GRANT LYTHE AND CARMEN MOLINA-PARÍS

DEPARTMENT OF APPLIED MATHEMATICS, UNIVERSITY OF LEEDS, LS29JT UK

Abstract. We consider diffusion in a disk, representing a cell with a circular interior compartment. Using bipolar coordinates, we perform exact calculations, not restricted by the size or location of the intracellular compartment. We find Green functions, hitting densities and mean times to move from the compartment to the cellular surface, and vice versa. For molecules with diffusivity D , mean times are proportional to R^2/D , where R is the radius of the cell. We find explicit expressions for the dependence on a^2 (the fraction of the cell occupied by the intracellular compartment) and on the displacement of the compartment from the center of the cell. We consider distributions of initial conditions that are (i) uniform on the nuclear surface, (ii) uniform on the cellular surface, or (iii) given by the hitting density of particles diffusing from the nuclear to the cellular surface.

1. Introduction. Living cells contain many proteins in ceaseless motion [1, 2]. The mechanism for responding to an event occurring on a cellular surface may involve the transport of molecular complexes to the nucleus [3–5], or of synthesised molecules from the nuclear to the cellular surface. Here, we consider transport that is simply diffusive, not accelerated by directed mechanisms or localised pathways, in a disk with an internal compartment. With the motivation of cell biology in mind, we refer to the boundary of the domain as the cellular surface and the internal compartment as the nucleus. We consider transport from a reflecting nuclear surface to an absorbing cellular surface, and back.

In many applications, the rate of contacts between diffusing reactants is calculated by solving the diffusion equation with appropriate boundary conditions [6–8]. Green’s function is the key to an analytical solution because quantities such as mean hitting times are obtained from it by standard integration, for any initial distribution [9–16]. Hitting times are important in other contexts, such as animal predators locating prey [17–19] and immunology, where encounters of T cells and antigen-presenting cells inside lymph nodes [20–26] trigger the adaptive immune response.

On a domain bounded by concentric circles, Green’s function can be found, as a series, using the reflection principle [27]. However, when the centres of the nucleus and cell do not coincide, exact solution has not been possible using cartesian or polar coordinates [18, 28]. An expression can be found using bipolar coordinates [29], in the case where the nuclear and cellular surfaces are both absorbing [30–32]. Transforming to bipolar coordinates is an example of a conformal mapping [32–34]. We consider, firstly, diffusive transport from the nucleus to the surface (reflecting nuclear surface, absorbing cellular surface) and, secondly, diffusive transport from the cellular surface to the nucleus (reflecting cellular surface, absorbing nuclear surface).

The problem of searching for a target, or multiple targets, within a closed domain is of considerable interest. In two and three dimensions, Condamin *et al.* [35], constructed approximate Green functions as a sum of pseudo-Green functions. A related problem is that of “narrow escape”, where a surface is reflecting everywhere except for a small hole [34, 36–38]. These analyses share the mathematical feature of a perturbation that is localised in space [25, 39–44]. Kurella *et al.* [18] have devised a hybrid asymptotic-numerical method to calculate mean times, and second moments, when there are multiple targets of different shapes in a two-dimensional region, accurate when the targets are not too large, not too close to each other and not too close to the cellular surface. Here, our calculations yield new, exact and explicit series expressions, on a disk with a *single* circular inclusion, independent of its size and position.

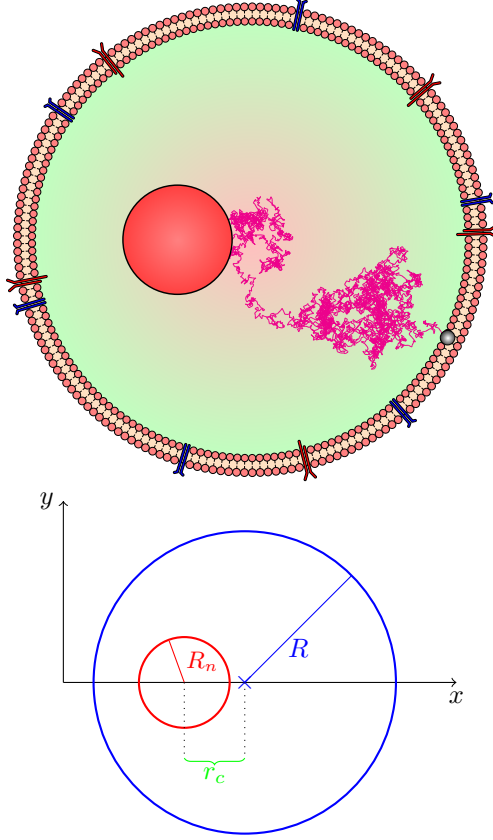


FIG. 1. We represent a cell as a circle of radius R , containing a nucleus of radius R_n . The center of the nucleus is displaced from that of the cell by r_c .

1.1. Geometry and coordinates. A circle of radius R (the cellular surface), contains a circle of radius R_n (the nuclear surface). The center of the nucleus is displaced from that of the cell by a distance r_c , as illustrated in Figure 1. We define the dimensionless quantities

$$a = \frac{R_n}{R} \quad \text{and} \quad c = \frac{r_c}{R},$$

that characterise the geometry. That is, we rescale lengths so that the radius of the cell is equal to 1. Note that $0 \leq c \leq 1 - a$, and a^2 is the fraction of the cell occupied by the nucleus. We denote the nuclear surface (a circle of scaled radius a , red in Figure 3) by ∂C_1 and the cellular surface (blue in Figure 3) by ∂C_2 .

We will use bipolar coordinates (τ, σ) , which are defined [18, 30] in terms of two foci whose separation is $2F$, as shown in Figure 2. In these coordinates, circles become curves of constant τ ; a circle of radius r is centred at $(\sqrt{r^2 + F^2}, 0)$, where $\tau = \log(F/r + \sqrt{1 + (F/r)^2})$. To represent our geometry, we place the foci so that the centres of the circles with radii 1 and a are displaced by c . That is, $c = \sqrt{1 + d^2} - \sqrt{a^2 + d^2}$. Thus, $d = \frac{F}{R}$ is given by

$$(1.1) \quad d = \frac{1}{2c} \sqrt{(1 + a^2 - c^2)^2 - 4a^2}.$$

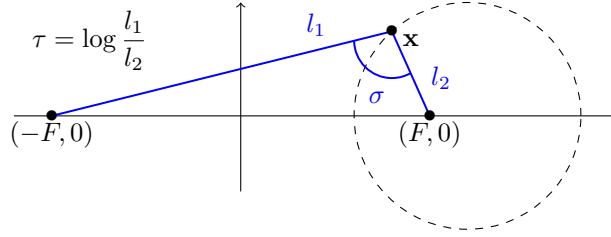


FIG. 2. The bipolar coordinates, τ and σ , of the point \mathbf{x} . The foci are at $(-F, 0)$ and $(F, 0)$.

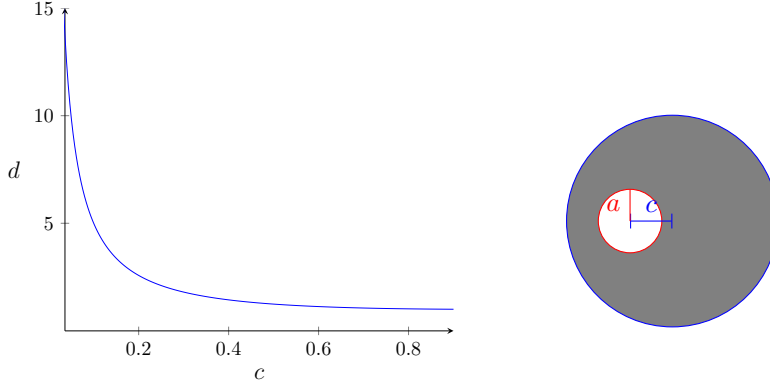


FIG. 3. Left: the rescaled interfocal distance d as a function of the displacement of the nucleus, c , when $a = 0.1$. Right: the domain C is shown in grey.

Hence, the eccentric annular region C (grey in Figure 3) is represented by [32]

$$\tau_2 < \tau < \tau_1, \quad 0 \leq \sigma < 2\pi,$$

where $\tau_1 = \log\left(\frac{d}{a} + \sqrt{1 + (d/a)^2}\right)$ (nuclear surface) and $\tau_2 = \log(d + \sqrt{1 + d^2})$ (cellular surface). In other words, we have

$$(1.2) \quad d = a \sinh \tau_1 = \sinh \tau_2.$$

A point \mathbf{x}_0 in C has dimensionless coordinates $\left(\frac{d \sinh \tau_0}{\cosh \tau_0 - \cos \sigma_0} - \sqrt{1 + d^2}, \frac{d \sin \sigma_0}{\cosh \tau_0 - \cos \sigma_0}\right)$ relative to the centre of the cell.

1.2. Green's function and mean times. Starting from $\mathbf{x}_0 \in C$, the mean time T to reach an absorbing boundary of the domain C , satisfies

$$(1.3) \quad \frac{D}{R^2} \Delta_{\mathbf{x}_0} T = -1.$$

In terms of Green's function, $G(\mathbf{x}_0, \mathbf{x})$,

$$(1.4) \quad T(\mathbf{x}_0) = \frac{R^2}{D} \int_C G(\mathbf{x}_0, \mathbf{x}) d\mathbf{x},$$

where $G(\mathbf{x}_0, \mathbf{x})$ satisfies

$$(1.5) \quad \Delta_{\mathbf{x}} G(\mathbf{x}_0, \mathbf{x}) = -\delta(\mathbf{x} - \mathbf{x}_0) \quad \mathbf{x} \in C,$$

with conditions on the boundaries of C . Let (τ, σ) be the bipolar coordinate representation of \mathbf{x} and (τ_0, σ_0) the representation of \mathbf{x}_0 . In bipolar coordinates,

$$d^2 \Delta_{\mathbf{x}} = (\cosh \tau - \cos \sigma)^2 \left(\frac{\partial^2}{\partial \tau^2} + \frac{\partial^2}{\partial \sigma^2} \right),$$

and we can write

$$(1.6) \quad T(\mathbf{x}_0) = \frac{R^2}{D} \int_{\tau_2}^{\tau_1} \int_0^{2\pi} \frac{G(\mathbf{x}_0, \mathbf{x}) d^2}{(\cosh \tau - \cos \sigma)^2} d\sigma d\tau.$$

2. Transport from the nuclear surface to the cellular surface. We begin with the case of diffusion with absorption on the cellular surface. Green's function, denoted in this case by G_1 , satisfies (1.5), is equal to zero on the cellular surface and has vanishing normal derivative on the nuclear surface. That is, we impose the following boundary conditions:

$$(2.1) \quad \begin{aligned} G_1(\mathbf{x}_0, \mathbf{x}) &= 0, & \mathbf{x} \in \partial C_2, \\ \frac{\partial G_1}{\partial \mathbf{n}_1}(\mathbf{x}_0, \mathbf{x}) &= 0, & \mathbf{x} \in \partial C_1, \end{aligned}$$

where \mathbf{n}_1 is normal to ∂C_1 . We can decompose G_1 into singular and regular (smooth) parts [9, 11, 27]:

$$(2.2) \quad 2\pi G_1(\mathbf{x}_0, \mathbf{x}) = 2\pi G_r(\mathbf{x}_0, \mathbf{x}) + \log \frac{1}{|\mathbf{x} - \mathbf{x}_0|},$$

where $\Delta_{\mathbf{x}} G_r(\mathbf{x}_0, \mathbf{x}) = 0$. Let $\tau_m = \min(\tau, \tau_0)$ and $\tau_M = \max(\tau, \tau_0)$. We use the following expression in bipolar coordinates [29, 30]:

$$(2.3) \quad \log \frac{1}{|\mathbf{x} - \mathbf{x}_0|} = \tau_m - \log 2d + \sum_{n=1}^{+\infty} \frac{1}{n} H_n(\mathbf{x}_0, \mathbf{x}),$$

where

$$H_n(\mathbf{x}_0, \mathbf{x}) = e^{-n|\tau - \tau_0|} \cos n(\sigma - \sigma_0) - e^{-n\tau} \cos n\sigma - e^{-n\tau_0} \cos n\sigma_0.$$

Our task is to find $G_r(\mathbf{x}_0, \mathbf{x})$, and hence $G_1(\mathbf{x}_0, \mathbf{x})$, in bipolar coordinates. The function is periodic in σ with boundary conditions at τ_1 and τ_2 [33]. We make use of the boundary conditions (2.1) to obtain

$$\begin{aligned} G_r(\mathbf{x}, \mathbf{x}_0) &= -\tau_2 + \log 2d + \sum_{n=1}^{+\infty} \frac{1}{n} (e^{-n\tau} \cos n\sigma + e^{-n\tau_0} \cos n\sigma_0) \\ &\quad - \sum_{n=1}^{+\infty} \frac{1}{n} \frac{\cos n(\sigma - \sigma_0)}{\cosh n(\tau_1 - \tau_2)} \left(\cosh n(\tau_1 - \tau_0) e^{-n(\tau - \tau_2)} - \sinh n(\tau_0 - \tau_2) e^{-n(\tau_1 - \tau)} \right). \end{aligned}$$

As a result, G_1 takes the convenient explicit form:

$$(2.4) \quad 2\pi G_1(\mathbf{x}_0, \mathbf{x}) = \tau_m - \tau_2 + \sum_{n=1}^{+\infty} \frac{2}{n} \cos n(\sigma - \sigma_0) K_1(n),$$

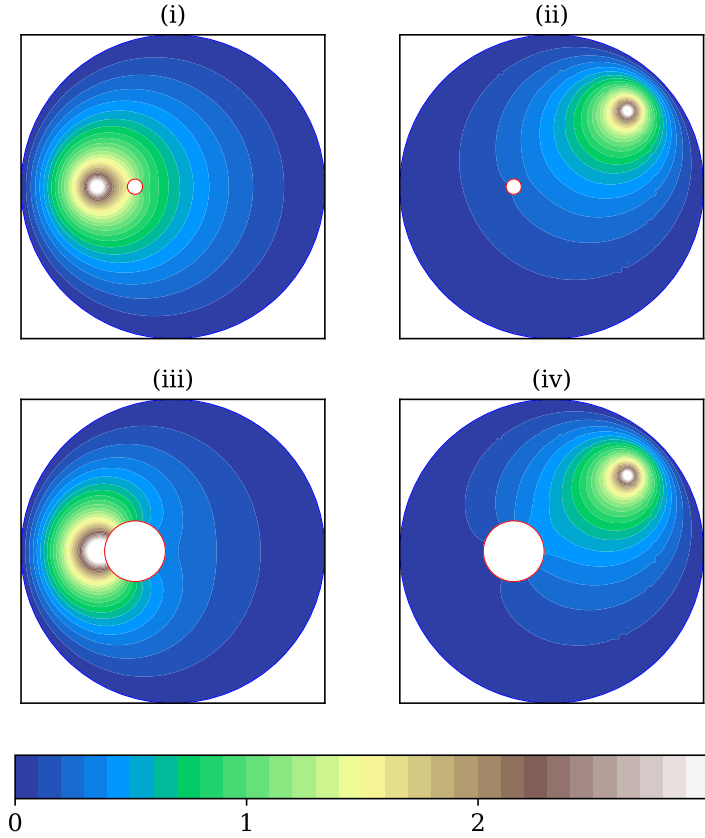


FIG. 4. Green's function (2.4) with reflecting nuclear surface and absorbing cellular surface. Four cases are shown: (i) $c = 0.25$, $a = 0.05$, $\mathbf{x}_0 - \mathbf{x}_c = (-0.25, 0)$. (ii) $c = 0.25$, $a = 0.05$, $\mathbf{x}_0 - \mathbf{x}_c = (0.75, 0.75)$. (iii) $c = 0.25$, $a = 0.2$, $\mathbf{x}_0 - \mathbf{x}_c = (-0.25, 0)$. (iv) $c = 0.25$, $a = 0.2$, $\mathbf{x}_0 - \mathbf{x}_c = (0.75, 0.75)$. Here \mathbf{x}_c is the position of the center of the cell.

where $K_1(n) = \sinh n(\tau_m - \tau_2) \frac{\cosh n(\tau_1 - \tau_M)}{\cosh n(\tau_1 - \tau_2)}$. We typically need at least 10 terms for accurate evaluation of G_1 , somewhat more as c approaches $1 - a$. To resolve the fine details in Figure 4, we used the first 100 terms in the series (2.4).

The method of images [45], illustrated in Fig. 5, yields a Green function $G_0(\mathbf{x}_0, \mathbf{x})$, with absorbing cellular surface but without nucleus (the case $a = 0$). Next, we use our exact expression to find an approximation, for the case of a small inclusion, that converges to G_0 as $a \rightarrow 0$. If the bipolar coordinates of the image point $\tilde{\mathbf{x}}_0$ (located outside C) are $(\tilde{\tau}_0, \tilde{\sigma}_0)$ then $\tau_0 + \tilde{\tau}_0 = 2\tau_2$ and

$$\begin{aligned} 2\pi G_0(\mathbf{x}_0, \mathbf{x}) &= \log |\mathbf{x} - \tilde{\mathbf{x}}_0| - \log |\mathbf{x} - \mathbf{x}_0| + \log r_0 \\ &= \tau_m - \tau_2 + \sum_{n=1}^{+\infty} \frac{2}{n} \cos n(\sigma - \sigma_0) K_0(n), \end{aligned}$$

where $K_0(n) = \sinh n(\tau_m - \tau_2) e^{-n(\tau_M - \tau_2)}$. As $a \rightarrow 0$, $\exp(\tau_2 - \tau_1) \rightarrow a/(1 - c^2)$ and

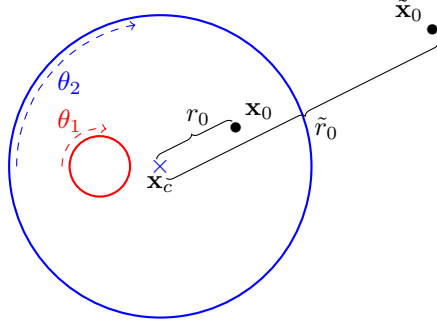


FIG. 5. The distance from \mathbf{x} to \mathbf{x}_c is r_0 . The image point $\tilde{\mathbf{x}}_0$ is defined such that $r_0 \tilde{r}_0 = 1$.

$G_1(\mathbf{x}_0, \mathbf{x})$ can be written as the sum of $G_0(\mathbf{x}_0, \mathbf{x})$ and corrections proportional to a^2 :

$$G_1(\mathbf{x}_0, \mathbf{x}) = G_0(\mathbf{x}_0, \mathbf{x}) + \frac{2a^2}{\pi(1-c^2)^2} \sinh(\tau - \tau_2) \sinh(\tau_0 - \tau_2) \cos(\sigma - \sigma_0) + \mathcal{O}(a^4).$$

In the concentric case $c = 0$,

$$2\pi G_1(\mathbf{x}_0, \mathbf{x}) = \log |\mathbf{x} - \tilde{\mathbf{x}}_0| - \log |\mathbf{x} - \mathbf{x}_0| + \log r_0 \\ + a^2 \cos(\theta - \theta_0) \left(\frac{1}{|\mathbf{x}|} - |\mathbf{x}| \right) \left(\frac{1}{|\mathbf{x}_0|} - |\mathbf{x}_0| \right) + \mathcal{O}(a^4).$$

3. Transport from cellular surface to nucleus. We turn to the case of diffusion from the cellular surface to an absorbing nucleus, and denote Green's function by $G_2(\mathbf{x}_0, \mathbf{x})$. It satisfies (1.5) with boundary conditions:

$$(3.1) \quad \begin{aligned} G_2(\mathbf{x}_0, \mathbf{x}) &= 0, & \mathbf{x} \in \partial C_1, \\ \frac{\partial G_2}{\partial \mathbf{n}_2}(\mathbf{x}_0, \mathbf{x}) &= 0, & \mathbf{x} \in \partial C_2, \end{aligned}$$

where \mathbf{n}_2 is the normal vector to ∂C_2 . Following the same methodology as in Section 2, we find

$$(3.2) \quad 2\pi G_2(\mathbf{x}_0, x) = \tau_1 - \tau_M + \sum_{n=1}^{+\infty} \frac{2}{n} \cos n(\sigma - \sigma_0) K_2(n),$$

where $K_2(n) = \sinh n(\tau_1 - \tau_M) \frac{\cosh n(\tau_m - \tau_2)}{\cosh n(\tau_1 - \tau_2)}$, $\tau_m = \min(\tau, \tau_0)$ and $\tau_M = \max(\tau, \tau_0)$.

In Figure 6, the exact Green function is compared with the approximation, accurate as $a \rightarrow 0$, of Condamin *et al.* [35], which was constructed as a sum of pseudo-Green functions, satisfying (1.5) but not satisfying the boundary condition on ∂C_1 . The resulting error is proportional to $a^2/(1-c^2)^2$ [46].

4. Hitting density on the cellular surface. Apart from mean times, Green functions are also used to calculate the densities of arrival positions on absorbing surfaces [10]. Consider molecules that are released from the nucleus and diffuse until they arrive at the cellular surface, ∂C_2 . With the exact Green function, we can calculate mean times and hitting densities for any initial condition or set of initial conditions.

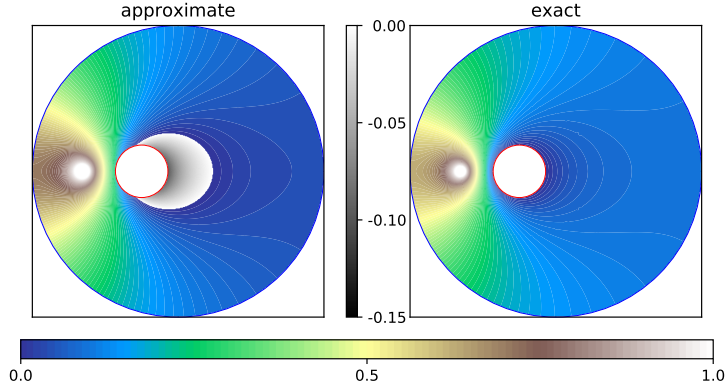


FIG. 6. *Exact Green function (3.2), with reflecting cellular surface and absorbing nuclear surface, and the approximation of Condamin et al. [35], which is negative on part of the domain that is shown in grey. $c = 0.25$, $a = 0.18$, $\mathbf{x}_0 - \mathbf{x}_c = (-0.65, 0)$.*

In this Section, we suppose that molecules may be released from anywhere on the nuclear surface, with the Cartesian angle θ_1 (see Figure 5) random and uniformly distributed in $(0, 2\pi)$. Accordingly, we integrate G_1 over ∂C_1 to define

$$P(\mathbf{x}) = \frac{1}{2\pi a} \int_{\partial C_1} G_1(\mathbf{x}_0, \mathbf{x}) d\mathbf{x}_0.$$

The density of the arrival, or hitting, point on the cellular surface is minus the outward normal derivative of $P(x)$. Using (2.4), we express the density as a function of the angle θ_2 on the cellular surface (see Figure 5):

$$(4.1) \quad \varepsilon(\theta_2) = - \left. \frac{\partial P(\mathbf{x})}{\partial \mathbf{n}_2} \right|_{\partial C_2} = \frac{\cosh \tau_2 - \cos \sigma_2}{2\pi d} \left(1 + \sum_{n=1}^{+\infty} \frac{2e^{-n\tau_1} \cos n\sigma_2}{\cosh n(\tau_1 - \tau_2)} \right).$$

The coordinate σ_2 is a function of θ_2 given by

$$(4.2) \quad \tan \sigma_2 = d \sin \theta_2 / (1 - \sqrt{1 + d^2} \cos \theta_2).$$

In summary, the distribution of values of θ_1 , the initial angle on the nuclear surface, is uniform but the distribution of values of θ_2 , the angle of arrival on the cellular surface, is not. In fact, if the nucleus is sufficiently displaced from the cell centre, then the distribution of values of θ_2 is bimodal (Figure 7).

5. Mean transport times. We now use the formula (1.6). Let $T_1(\theta_1)$ be the mean time to reach the cellular surface, starting on a reflecting nuclear surface; the initial point $\mathbf{x}_0 \in \partial C_1$ is specified by the angle θ_1 (see Figure 5). We write

$$\begin{aligned} T_1(\theta_1) &= \frac{R^2 d^2}{D} \int_{\tau_2}^{\tau_1} \int_0^{2\pi} \frac{G_1(\mathbf{x}_0, \mathbf{x})}{(\cosh \tau - \cos \sigma)^2} d\sigma d\tau \\ &= \frac{R^2 d^2}{2\pi D} \int_{\tau_2}^{\tau_1} \int_0^{2\pi} \frac{\tau - \tau_2}{(\cosh \tau - \cos \sigma)^2} d\sigma d\tau \\ &\quad + \sum_{n=1}^{+\infty} \frac{R^2 d^2}{n\pi D} \int_{\tau_2}^{\tau_1} K_1(n) \int_0^{2\pi} \frac{\cos n(\sigma - \sigma_1)}{(\cosh \tau - \cos \sigma)^2} d\sigma d\tau, \end{aligned}$$

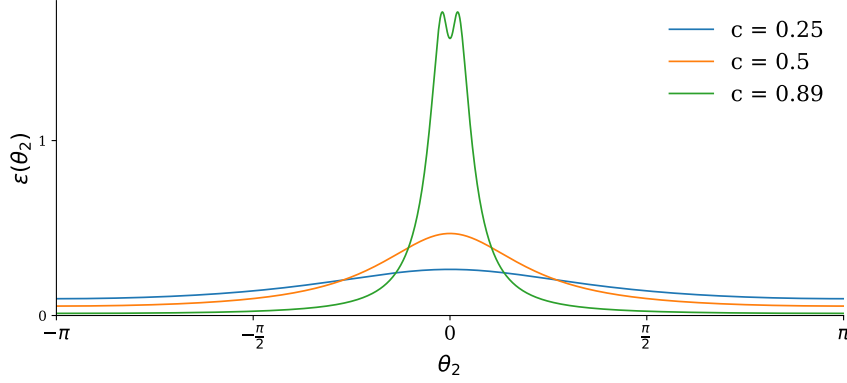


FIG. 7. The density of the first hitting point on the cellular surface, (4.1), when the initial condition is uniformly distributed on the nuclear surface. The nucleus has radius $a = 0.1$ and c is the distance of its centre from the centre of the cell.

and $\tan \sigma_1 = d \sin \theta_1 / (a - \sqrt{a^2 + d^2} \cos \theta_1)$. Using (A.3) and the relationships

$$d^2 (\coth \tau_2 - \coth \tau_1) = dc \quad \text{and} \quad a \sinh(\tau_1 - \tau_2) = dc,$$

we find

$$(5.1) \quad \frac{2D}{R^2} T_1(\theta_1) = dc - a^2(\tau_1 - \tau_2) + 4 \sum_{n=1}^{+\infty} \frac{\cos n\sigma_1}{e^{n\tau_1}} \times \left(\frac{dc}{1 + e^{-2n(\tau_1 - \tau_2)}} - \frac{a^2}{2n} \tanh n(\tau_1 - \tau_2) \right).$$

Let $T_2(\theta_2)$ be the mean time to reach the nuclear surface, starting at θ_2 on a reflecting cellular surface. Then

$$(5.2) \quad \frac{2D}{R^2} T_2(\theta_2) = \tau_1 - \tau_2 - dc - 4 \sum_{n=1}^{+\infty} \frac{\cos n\sigma_2}{e^{n\tau_2}} \times \left(\frac{dc}{1 + e^{2n(\tau_1 - \tau_2)}} - \frac{1}{2n} \tanh n(\tau_1 - \tau_2) \right).$$

The dependence on θ_2 is shown in Figure 8 for six different combinations of a and c . The dotted lines are

$$(5.3) \quad \frac{2D}{R^2} T_2(\theta_2) \simeq \log \frac{1}{a(1-c^2)} - \frac{1}{2}(1-c^2) + \log((\cos \theta_2 - c)^2 + \sin^2 \theta_2),$$

obtained from principal result 2.2 of Kurella *et al.* [18].

As in Section 4, we are interested in the situation where molecules can be released from any part of the initial surface. Thus we desire the mean hitting times when the initial angles (θ_1 or θ_2) are uniformly distributed. We indicate these times by an overbar and make explicit that they are functions of a and c . Firstly, when the initial position is uniform on the nuclear surface,

$$(5.4) \quad \bar{T}_1(a, c) = \int_0^{2\pi} \frac{T_1(\theta_1)}{2\pi a} d\theta_1 = \frac{d}{2\pi a} \int_0^{2\pi} \frac{T_1(\theta_1)}{\cosh \tau_1 - \cos \sigma_1} d\sigma_1.$$

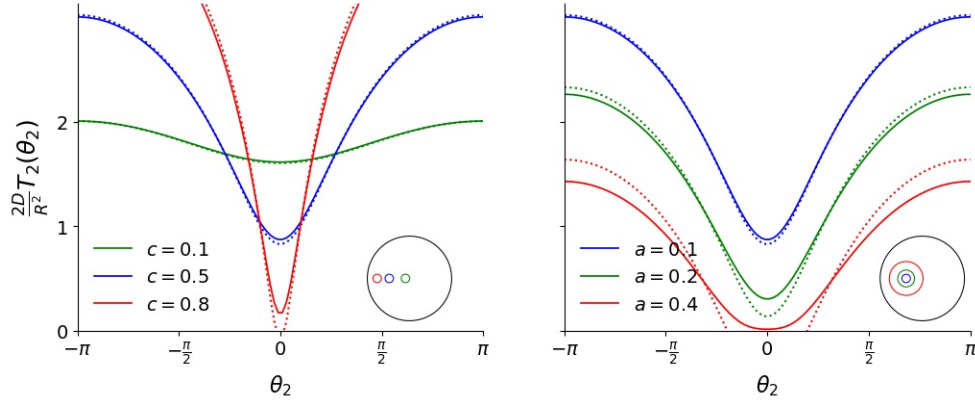


FIG. 8. The mean time (5.2) to hit the nucleus, starting at a point on the cellular surface parametrised by θ_2 . On the left, for three different values of c , with $a = 0.1$ fixed. On the right, for three different values of a , with $c = 0.5$ fixed. Dotted lines are the approximation (5.3). Disks and three different inclusions are illustrated at bottom right in each panel.

Using (A.2) and the identities (1.2), we find

$$(5.5) \quad \frac{2D}{R^2} \bar{T}_1(a, c) = dc - a^2(\tau_1 - \tau_2) + 4 \sum_{n=1}^{+\infty} e^{-2n\tau_1} \times \left(\frac{dc}{1 + e^{-2n(\tau_1 - \tau_2)}} - \frac{a^2}{2n} \tanh n(\tau_1 - \tau_2) \right).$$

The dependence on a and c is shown in Figure 9.

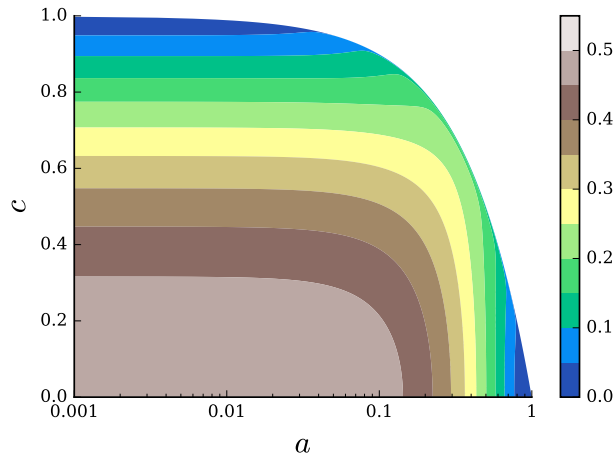


FIG. 9. Contours of $\frac{2D}{R^2} \bar{T}_1$, the mean time for a particle, whose initial condition is uniformly distributed on the nuclear surface, to reach the cellular surface, as a function of the dimensionless parameters a and c .

Similarly, the mean time for a particle, whose initial condition is uniformly dis-

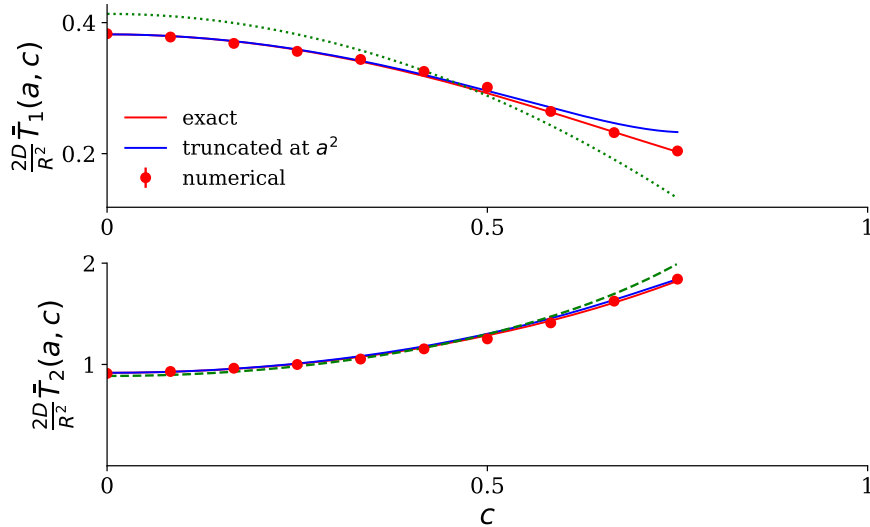


FIG. 10. Mean times as a function of c , with $a = 0.25$. In the upper panel, the mean time to hit the cellular surface when the initial condition is uniformly distributed on the nuclear surface. In the lower panel, the mean time to hit the nuclear surface when the initial condition is uniformly distributed on the cellular surface. Red lines: exact formulae (5.5) and (5.6). Blue lines: (5.7) and (5.8), including terms up to $\mathcal{O}(a^2)$ only. Dashed green lines: lowest-order approximations, $\frac{2D}{R^2}\bar{T}_1 \simeq \frac{1}{2}(1-c^2) + a^2 \log a$ and $\frac{2D}{R^2}\bar{T}_2 \simeq \log \frac{1}{a(1-c^2)} - \frac{1}{2}(1-c^2)$. Red dots: averages over numerically-generated realisations.

tributed on the cellular surface, to reach the nucleus is given by

$$(5.6) \quad \frac{2D}{R^2}\bar{T}_2(a, c) = \tau_1 - \tau_2 - dc - 4 \sum_{n=1}^{+\infty} e^{-2n\tau_2} \times \left(\frac{dc}{1 + e^{2n(\tau_1 - \tau_2)}} - \frac{1}{2n} \tanh n(\tau_1 - \tau_2) \right).$$

It is instructive to expand these mean times in powers of a^2 :

$$(5.7) \quad \frac{2D}{R^2}\bar{T}_1(a, c) = \frac{1}{2}(1 - c^2) - a^2 \log \frac{1 - c^2}{a} - \frac{a^2}{2} \left(1 - \frac{2c^2}{1 - c^2} \right) + \mathcal{O}(a^4)$$

and

$$(5.8) \quad \frac{2D}{R^2}\bar{T}_2(a, c) = \log \frac{1}{a(1 - c^2)} - \frac{1}{2}(1 - c^2) + \frac{a^2}{2} \left(1 - \frac{2c^2}{(1 - c^2)^2} \right) + \mathcal{O}(a^4).$$

The $\mathcal{O}(a^4)$ terms are zero when $c = 0$. Performing the integral (1.4) using the approximate Green function of Condamin *et al.* [35] yields the first two terms of (5.8), shown as the dashed line in Figure 10. The latter is a rather good approximation at $a = 0.25$, but worsening as the nucleus approaches the cellular surface. Also shown is the approximation obtained by retaining terms proportional to a^2 in (5.8). The red dots are numerical average times obtained from Brownian paths starting on one, reflecting, surface and ending on the other, absorbing surface.

We end this Section by considering the mean time that is obtained by averaging over all possible positions of the nucleus. The results, functions of a only, are

$$(5.9) \quad \frac{2D}{R^2} \bar{T}_1(a) = \frac{2}{(1-a)^2} \int_0^{1-a} c \bar{T}_1(a, c) dc = \frac{1}{4} + \frac{1}{2}a - \left(\frac{3}{4} + \log 2\right) a^2 + \mathcal{O}(a^3)$$

and

$$(5.10) \quad \frac{2D}{R^2} \bar{T}_2(a) = (1 - 2a - 2a^2) \log \frac{1}{a} + \frac{3}{4} + (1 + \log 2)a + (\log 2)a^2 + \mathcal{O}(a^3).$$

We note that $\bar{T}_1(a)$ is a non-monotonic function of a , with maximum at $a \approx 0.173$.

6. Mean round-trip time. We now calculate the mean time for a particle to diffuse outward to the cellular surface and, from there, inward back to the nucleus. The initial condition is distributed uniformly on the nuclear surface; the end point of the outward path (on the cellular surface) is the starting point of the inward path. This affects the inward leg; instead of an initial condition distributed uniformly on the cellular surface, we use the hitting density, calculated in Section 4, as the initial distribution. That is,

$$(6.1) \quad \bar{T}_2^\varepsilon(a, c) = \int_0^{2\pi} \varepsilon(\theta_2) T_2(\theta_2) d\theta_2.$$

The functions in the integrand have been expanded in (4.1) and (5.2) using the variable σ_2 , given by (4.2). Similarly, we can expand the integrand of (6.1) as the Fourier-cosine series:

$$\varepsilon(\theta_2) T_2(\theta_2) = \frac{R^2}{2D} \frac{1}{2\pi} \left(C_0 + \sum_{n=1}^{+\infty} C_n \cos n\sigma_2 \right).$$

Then

$$(6.2) \quad \begin{aligned} \frac{2D}{R^2} \bar{T}_2^\varepsilon(a, c) &= \frac{d}{2\pi} \int_0^{2\pi} \frac{C_0 + \sum_{n=1}^{+\infty} C_n \cos n\sigma_2}{\cosh \tau_2 - \cos \sigma_2} d\sigma_2 \\ &= C_0 + \sum_{n=1}^{+\infty} e^{-n\tau_2} C_n. \end{aligned}$$

The mean round-trip time, plotted in Figure 11, is the sum, $\bar{T}_1(a, c) + \bar{T}_2^\varepsilon(a, c)$.

7. Direct solution of Poisson's equation. An alternative way to find mean transport times, still in bipolar coordinates but without first calculating Green functions, is to solve Poisson's equation (1.3). We first consider the mean time $T_3(\mathbf{x}_0)$ to the cellular surface, starting from $\mathbf{x}_0 \in C$. The boundary conditions are

$$T_3|_{\tau_0=\tau_2} = 0 \quad \frac{\partial}{\partial \tau_0} T_3 \Big|_{\tau_0=\tau_1} = 0 \quad \frac{\partial}{\partial \sigma_0} T_3 \Big|_{\sigma_0=0, \pi} = 0.$$

We recognise the particular solution

$$(7.1) \quad T_3^p(\mathbf{x}_0) = -\frac{R^2 d^2}{2D} \frac{\cosh \tau_0}{\cosh \tau_0 - \cos \sigma_0},$$

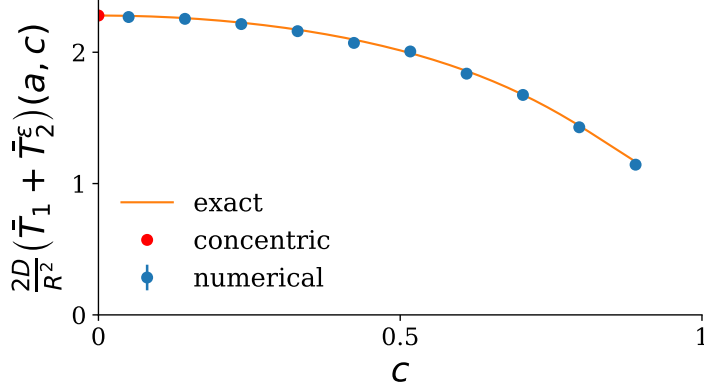


FIG. 11. Mean round-trip time $\bar{T}_1(a, c) + \bar{T}_2^\varepsilon(a, c)$ as a function of c , with $a = 0.1$. The line is the sum of the analytic results (5.5) and (6.2). The blue dots are numerical simulations and the red dot is $\bar{T}_1(a, 0) + \bar{T}_2^\varepsilon(a, 0) = \frac{R^2}{2D}(1 - a^2) \log \frac{1}{a}$.

and write

$$(7.2) \quad T_3(\mathbf{x}_0) = A\tau_0 + B + \sum_{n=1}^{+\infty} (C_n e^{n\tau_0} + D_n e^{-n\tau_0}) \cos n\sigma_0 - \frac{R^2 d^2}{2D} \frac{\cosh \tau_0}{\cosh \tau_0 - \cos \sigma_0}.$$

Using the identity

$$\frac{\cosh \tau}{\cosh \tau - \cos \sigma} = \coth \tau \left(1 + 2 \sum_{n=1}^{+\infty} e^{-n\tau} \cos n\sigma \right),$$

we find

$$(7.3) \quad \begin{aligned} \frac{2D}{R^2} T_3(\mathbf{x}_0) &= d^2 (\coth \tau_2 - \coth \tau_0) - a^2 (\tau_0 - \tau_2) \\ &\quad + 2d^2 \sum_{n=1}^{+\infty} (J_n(\tau_0, \tau_1, \tau_2) - \coth \tau_0 e^{-n\tau_0}) \cos n\sigma_0, \end{aligned}$$

where

$$(7.4) \quad \begin{aligned} J_n(\tau_0, \tau_1, \tau_2) &= \frac{e^{-n\tau_1} \sinh n(\tau_2 - \tau_0)}{\cosh n(\tau_2 - \tau_1)} \left(\frac{1}{n \sinh^2 \tau_1} + \coth \tau_1 \right) \\ &\quad + \frac{\coth \tau_2 e^{-n\tau_2}}{\cosh n(\tau_2 - \tau_1)} \cosh n(\tau_1 - \tau_0). \end{aligned}$$

Similarly, the mean time $T_4(\mathbf{x}_0)$ to the nuclear surface, starting from $\mathbf{x}_0 \in C$, with the cellular surface reflecting, is

$$(7.5) \quad \begin{aligned} \frac{2D}{R^2} T_4(\mathbf{x}_0) &= \tau_1 - \tau_0 - d^2 (\coth \tau_0 - \coth \tau_1) \\ &\quad + 2d^2 \sum_{n=1}^{+\infty} (J_n(\tau_0, \tau_2, \tau_1) - \coth \tau_0 e^{-n\tau_0}) \cos n\sigma_0. \end{aligned}$$

8. Discussion. We perform exact calculations that, until now, have only been possible using approximations or asymptotics. The mean time to reach the cellular surface, starting at $\mathbf{x}_0 \in C$ with reflecting nuclear surface, is given by (7.3); the mean time to reach the nuclear surface, with reflecting cellular surface, is given by (7.5). These results, and the exact Green functions, (2.4) and (3.2), are obtained using bipolar coordinates. In the appropriate limits, our results agree with those in Condamin *et al.* [35], and Kurella *et al.* [18], obtained using either psuedo-Green functions or matched asymptotic analysis. Our method provides an exact solution even when the nucleus is close to the cell boundary, where other methods fail. However, extending our analysis to the case of partially-reflecting boundaries will be complicated by the appearance of a Jacobian, and exact analysis does not appear possible if the diffusivity is position-dependent.

Once Green’s function is known, we can calculate mean times for any set of initial conditions. In Section 2, we analyse the case where the initial position is a given point on the nuclear surface, and the case where it is randomly-distributed on the nuclear surface. In Section 3, we analyse the case where the initial position is a given point on the cellular surface, and the case where it is randomly-distributed on the cellular surface. The motivation is to model diffusive transport under the assumption the location on the surface of an intracellular compartment where a molecule emerges, or on the cellular surface where a molecular complex is internalised, is uniformly distributed. The exact expressions for the hitting densities and mean arrival times are (4.1), (5.1) and (5.2). When averaged over the initial surface, the mean arrival times, (5.5) and (5.6), are functions of a and c . We perform a further averaging: over all possible locations of the nucleus within the cell, obtaining (5.9) and (5.10), functions of a only.

Bispherical coordinates can be used to undertake calculations, similar to those presented here, in three space dimensions [46]. However, finding mathematical descriptions of the traffic of small molecules inside living cells and of living cells in tissues presents challenges; Brownian motion is not sufficient [4, 26, 47–57]. For example, viral trajectories in the cytoplasm may be modelled as epochs of simple diffusion and of active transport along microtubules [2]. To molecules diffusing inside cells, intracellular compartments may be obstacles or targets. The molecules themselves may have finite lifetimes [5]. Effects of crowding or of active transport mechanisms may be modelled as a type of motion that is not diffusive, with the standard time derivative replaced by a fractional one [26, 54, 58]. A reacting surface may itself contain absorbing and reflecting regions [59]; one way to take this heterogeneity into account is via Robin boundary conditions [25].

Acknowledgements

RS acknowledges supported from the University of Leeds, Dstl and EPSRC as recipient of an EPSRC-Smith Institute ICASE studentship, DSTLX1000102046R.

Data Availability

The codes that support the findings of this study are openly available at <http://www1.maths.leeds.ac.uk/~grant/Green/>.

Appendix A. Evaluation of integrals.

We define

$$(A.1) \quad I_{n,k} = \int_0^{2\pi} \frac{\cos n(\sigma - \sigma_0)}{(\cosh \tau - \cos \sigma)^k} d\sigma = \cos n\sigma_0 \int_0^{2\pi} \frac{\cos n\sigma}{(\cosh \tau - \cos \sigma)^k} d\sigma.$$

If $z = e^{i\sigma}$ then $I_{n,k} = -i \cos n\sigma_0 \int_{|z|=1} f_{n,k}(z) dz$, where

$$f_{n,k}(z) = \frac{(2z)^k z^{n-1}}{(z - z_1)^k (z_2 - z)^k},$$

$z_1 = e^{-\tau}$ and $z_2 = e^{\tau}$. Thus, we have

$$\int_{|z|=1} f_{n,k}(z) dz = \frac{2\pi i}{(k-1)!} \frac{\partial^{k-1}}{\partial z^{k-1}} \left(\frac{z^{n-1} (2z)^k}{(z_2 - z)^k} \right) \Bigg|_{z=z_1}.$$

In particular,

$$(A.2) \quad I_{n,1}(\tau) = \frac{2\pi \cos n\sigma_0}{e^{n\tau} \sinh \tau}$$

and

$$(A.3) \quad I_{n,2}(\tau) = 2\pi \cos n\sigma_0 \frac{n \sinh \tau + \cosh \tau}{e^{n\tau} \sinh^3 \tau}.$$

REFERENCES

- [1] Conrad W Mullineaux, Anja Nenninger, Nicola Ray, and Colin Robinson. Diffusion of green fluorescent protein in three cell environments in escherichia coli. *Journal of Bacteriology*, 188(10):3442–3448, 2006.
- [2] Thibault Lagache, Emmanuel Dauty, and David Holcman. Quantitative analysis of virus and plasmid trafficking in cells. *Physical Review E*, 79(1):011921, 2009.
- [3] Björn F Lillemeier, Mario M Köster, and Ian M Kerr. STAT1 from the cell membrane to the DNA. *The EMBO Journal*, 20(10):2508–2517, 2001.
- [4] David Holcman. *Stochastic processes, multiscale modeling, and numerical methods for computational cellular biology*. Springer, 2017.
- [5] Denis S Grebenkov, Ralf Metzler, and Gleb Oshanin. Effects of the target aspect ratio and intrinsic reactivity onto diffusive search in bounded domains. *New Journal of Physics*, 19(10):103025, 2017.
- [6] Olivier Bénichou, C Chevalier, Joseph Klafter, B Meyer, and Raphael Voituriez. Geometry-controlled kinetics. *Nature Chemistry*, 2(6):472, 2010.
- [7] RK Michael Thambynayagam. *The diffusion handbook: applied solutions for engineers*. McGraw Hill Professional, 2011.
- [8] Katja Lindenberg, Ralf Metzler, and Gleb Oshanin, editors. *Chemical kinetics beyond the textbook*. World Scientific, 2019.
- [9] Gabriel Barton. *Elements of Green's functions and propagation: potentials, diffusion, and waves*. Oxford University Press, 1989.
- [10] Sidney Redner. *A guide to first-passage processes*. Cambridge University Press, 2001.
- [11] David Stirzaker et al. *Stochastic processes and models*. OUP Catalogue, 2005.
- [12] Matthew CM Wright. Green function or Green's function? *Nature Physics*, 2(10):646–646, 2006.
- [13] George B Arfken and Hans J Weber. *Mathematical methods for physicists*. Academic press, 7 edition, 2013.
- [14] Thorsten Prüstel and Martin Meier-Schellersheim. Exact Green's function of the reversible diffusion-influenced reaction for an isolated pair in two dimensions. *Journal of Chemical Physics*, 137(5):054104, 2012.
- [15] Thorsten Prüstel and M Tachiya. Reversible diffusion-influenced reactions of an isolated pair on some two dimensional surfaces. *Journal of Chemical Physics*, 139(19):194103, 2013.
- [16] Thorsten Prüstel and Martin Meier-Schellersheim. Theory of reversible diffusion-influenced reactions with non-Markovian dissociation in two space dimensions. *Journal of Chemical Physics*, 138(10):104112, 2013.
- [17] Hannah W McKenzie, Mark A Lewis, and Evelyn H Merrill. First passage time analysis of animal movement and insights into the functional response. *Bulletin of Mathematical Biology*, 71(1):107–129, 2009.

- [18] Venu Kurella, Justin C Tzou, Daniel Coombs, and Michael J Ward. Asymptotic analysis of first passage time problems inspired by ecology. *Bulletin of Mathematical Biology*, 77(1):83–125, 2015.
- [19] Melanie E Moses, Judy L Cannon, Deborah M Gordon, and Stephanie Forrest. Distributed adaptive search in T cells: Lessons from ants. *Frontiers in immunology*, 10:1357, 2019.
- [20] Paul Garside, Elizabeth Ingulli, Rebecca R. Merica, Julia G. Johnson, Randolph J. Noelle, and Marc K. Jenkins. Visualization of specific B and T lymphocyte interactions in the lymph node. *Science*, 281(5373):96, 1998.
- [21] Frederik W Wiegel and Alan S Perelson. Some scaling principles for the immune system. *Immunology and cell biology*, 82(2):127–131, 2004.
- [22] Bernd H Zinselmeyer, John Dempster, Alison M Gurney, David Wokosin, Mark Miller, Hsiang Ho, Owain R Millington, Karen M Smith, Catherine M Rush, Ian Parker, et al. In situ characterization of CD4⁺ T cell behavior in mucosal and systemic lymphoid tissues during the induction of oral priming and tolerance. *Journal of Experimental Medicine*, 201(11):1815–1823, 2005.
- [23] Susanna Celli, Mark Day, Andreas J Müller, Carmen Molina-Paris, Grant Lythe, and Philippe Bousso. How many dendritic cells are required to initiate a T-cell response? *Blood*, 120(19):3945–3948, 2012.
- [24] Johannes Textor, Sarah E Henrikson, Judith N Mandl, Ulrich H von Andrian, Jürgen Westermann, Rob J de Boer, and Joost B Beltman. Random migration and signal integration promote rapid and robust T cell recruitment. *PLoS Computational Biology*, 10(8):e1003752, 2014.
- [25] Monica I Delgado, Michael J Ward, and Daniel Coombs. Conditional mean first passage times to small traps in a 3-D domain with a sticky boundary: applications to T cell searching behavior in lymph nodes. *Multiscale Modeling & Simulation*, 13(4):1224–1258, 2015.
- [26] Matthew F Krummel, Frederic Bartumeus, and Audrey Gérard. T cell migration, search strategies and mechanisms. *Nature Reviews Immunology*, 16(3):193, 2016.
- [27] Richard Courant and David Hilbert. *Methods of mathematical physics*. CUP Archive, 1965.
- [28] Jeng-Tzong Chen, KH Chou, and SK Kao. Derivation of Greens function using addition theorem. *Mechanics Research Communications*, 36(3):351–363, 2009.
- [29] Philip M Morse and Herman Feshbach. *Methods of theoretical physics, Part II*. McGraw-Hill, 1953.
- [30] James F Heyda. A Green’s function solution for the case of laminar incompressible flow between non-concentric circular cylinders. *Journal of the Franklin Institute*, 267(1):25–34, 1959.
- [31] Jeng-Tzong Chen, Hungchih Shieh, Yingte Lee, and Jia-Wei Lee. Bipolar coordinates, image method and the method of fundamental solutions for Greens functions of Laplace problems containing circular boundaries. *Engineering Analysis with Boundary Elements*, 35(2):236–243, 2011.
- [32] André Liemert. The Green’s function of the Poisson equation on the non-concentric annular region. *Journal of Electrostatics*, 72(4):347–351, 2014.
- [33] Jeng-Tzong Chen, Ming-Hong Tsai, and Chein-Shan Liu. Conformal mapping and bipolar coordinate for eccentric Laplace problems. *Computer Applications in Engineering Education*, 17(3):314–322, 2009.
- [34] Denis S Grebenkov. Universal formula for the mean first passage time in planar domains. *Physical Review Letters*, 117(26):260201, 2016.
- [35] Sylvain Condamin, Olivier Bénichou, and Michel Moreau. Random walks and Brownian motion: A method of computation for first-passage times and related quantities in confined geometries. *Physical Review E*, 75(2):021111, 2007.
- [36] Zeev Schuss, Amit Singer, and David Holcman. The narrow escape problem for diffusion in cellular microdomains. *Proceedings of the National Academy of Sciences*, 104(41):16098–16103, 2007.
- [37] Amit Singer, Zeev Schuss, and David Holcman. Narrow escape, part II: The circular disk. *Journal of Statistical Physics*, 122(3):465–489, 2006.
- [38] David Holcman and Zeev Schuss. The narrow escape problem. *SIAM Review*, 56(2):213–257, 2014.
- [39] Micheal J Ward and Joseph B Keller. Strong localized perturbations of eigenvalue problems. *SIAM Journal on Applied Mathematics*, 53(3):770–798, 1993.
- [40] Theodore Kolokolnikov, Michele S Titcombe, and Michael J Ward. Optimizing the fundamental neumann eigenvalue for the Laplacian in a domain with small traps. *European Journal of Applied Mathematics*, 16(2):161–200, 2005.
- [41] Omer Dushek and Daniel Coombs. Analysis of serial engagement and peptide-MHC transport in T cell receptor microclusters. *Biophysical journal*, 94(9):3447–3460, 2008.

- [42] Daniel Coombs, Ronny Straube, and Michael J Ward. Diffusion on a sphere with localized traps: mean first passage time, eigenvalue asymptotics, and Fekete points. *SIAM Journal of Applied Math*, 70(1):302–332, 2009.
- [43] Samara Pillay, Michael J Ward, A Peirce, and Theodore Kolokolnikov. An asymptotic analysis of the mean first passage time for narrow escape problems: Part I: Two-dimensional domains. *Multiscale Modeling & Simulation*, 8(3):803–835, 2010.
- [44] Samuel A Isaacson and Jay Newby. Uniform asymptotic approximation of diffusion to a small target. *Physical Review E*, 88(1):012820, 2013.
- [45] John David Jackson. *Classical electrodynamics*. Wiley, 1999.
- [46] Remus Stana. *Diffusive transport: theory and application*. PhD thesis, University of Leeds, 2020.
- [47] Bastian R Angermann, Frederick Klauschen, Alex D Garcia, Thorsten Prustel, Fengkai Zhang, Ronald N Germain, and Martin Meier-Schellersheim. Computational modeling of cellular signaling processes embedded into dynamic spatial contexts. *Nature Methods*, 9(3):283, 2012.
- [48] Eli Barkai, Yuval Garini, and Ralf Metzler. Strange kinetics of single molecules in living cells. *Physics Today*, 65(8):29, 2012.
- [49] Thiago G Mattos, Carlos Mejía-Monasterio, Ralf Metzler, and Gleb Oshanin. First passages in bounded domains: When is the mean first passage time meaningful? *Physical Review E*, 86(3):031143, 2012.
- [50] Paul C Bressloff and Jay M Newby. Stochastic models of intracellular transport. *Reviews of Modern Physics*, 85(1):135, 2013.
- [51] Clifford P Brangwynne, Gijsje H Koenderink, Frederick C MacKintosh, and David A Weitz. Intracellular transport by active diffusion. *Trends in Cell Biology*, 19(9):423–427, 2009.
- [52] Maria R D’Orsogna and Tom Chou. Optimal cytoplasmic transport in viral infections. *PLoS ONE*, 4(12):e8165, 2009.
- [53] Sean R McGuffee and Adrian H Elcock. Diffusion, crowding and protein stability in a dynamic molecular model of the bacterial cytoplasm. *PLoS Computational Biology*, 6(3), 2010.
- [54] Ralf Metzler. Brownian motion and beyond: first-passage, power spectrum, non-gaussianity, and anomalous diffusion. *Journal of Statistical Mechanics: Theory and Experiment*, 2019(11):114003, 2019.
- [55] Denis S Grebenkov and J-F Rupprecht. The escape problem for mortal walkers. *Journal of Chemical Physics*, 146(8):084106, 2017.
- [56] Denis S Grebenkov, Ralf Metzler, and Gleb Oshanin. Towards a full quantitative description of single-molecule reaction kinetics in biological cells. *Physical Chemistry Chemical Physics*, 20(24):16393–16401, 2018.
- [57] Sean D Lawley and Christopher E Miles. Diffusive search for diffusing targets with fluctuating diffusivity and gating. *Journal of Nonlinear Science*, 29(6):2955–2985, 2019.
- [58] Kevin Burrage, Angelamaria Cardone, Raffaele D’Ambrosio, and Beatrice Paternoster. Numerical solution of time fractional diffusion systems. *Applied Numerical Mathematics*, 116:82–94, 2017.
- [59] C Chevalier, O Bénichou, B Meyer, and R Voituriez. First-passage quantities of brownian motion in a bounded domain with multiple targets: a unified approach. *Journal of Physics A: Mathematical and Theoretical*, 44(2):025002, 2010.